A Method for the Rapid Generation of Nonsequential Light-Response Curves of Chlorophyll Fluorescence

Joao Serôdio, Joao Ezequiel, Jörg Frommlet, Martin Laviale, Johann Lavaud

Running Head: Single pulse light curves

João Serôdio

Departamento de Biologia and CESAM – Centro de Estudos do Ambiente e do Mar,
Universidade de Aveiro, Campus de Santiago, 3810-193 Aveiro, Portugal
Tel: +351 234370787
E-mail: jserodio@ua.pt

Research area: Breakthrough Technologies

A method for the rapid generation of non-sequential light-response curves of chlorophyll fluorescence

João Serôdio[1], João Ezequiel[1], Jörg Frommlet[1], Martin Laviale[1], Johann Lavaud[2]

Address: [1]Departamento de Biologia and CESAM – Centro de Estudos do Ambiente e do Mar, Universidade de Aveiro, Campus de Santiago, 3810-193 Aveiro, Portugal; [2]UMR 7266 'LIENSs', CNRS-University of La Rochelle, Institute for Coastal and EnvironmentalResearch (ILE), 2 rue Olympe de Gouges, 17 000 La Rochelle, France

One-sentence summary: Light-response curves of chlorophyll fluorescence are rapidly generated from independent, non-sequential measurements through the combined use of spatially separated beams of actinic light and fluorescence imaging.

Financial source: This work was supported by the FCT – Fundaçãopara a Ciência e a Tecnologia, through grants SFRH/BSAB/962/2009 (J.Serôdio), SFRH/BD/44860/2008 (J. Ezequiel), and projectsMigROS (PTDC/MAR/112473/2009; M. Laviale),SeReZoox (PTDC/MAR/113962/2009; J. Frommlet), by the CNRS – Centre National de la RechercheScientifique (‘chercheursinvités’ program, J. Serôdio and J.Lavaud), and by the French consortium CPER-Littoral, and the Egide/Campus France PHC Pessoa exchange program (n°27377TB to J. Serôdio and J. Lavaud).

Corresponding author: João Serôdio, jserodio@ua.pt

Abstract

Light-response curves (LC) of chlorophyll fluorescenceare widely used in plant physiology. Most commonly, LCs are generated sequentially,exposing the same sample to a sequence of distinct actinic lightintensities. These measurements are not independent, as the response to each new light level is affected by the light exposure history experienced during previous steps of the LC, an issue particularly relevant in the case of the popular Rapid Light Curves.In this work we demonstrate the proof of concept of a new method for the rapid generation of LCs from non-sequential, temporally-independent fluorescence measurements. The method is based on the combined use of sample illumination with digitally controlled, spatially separated beams of actinic light, andof a fluorescence imaging system. It allows the generationof a whole LC, including a large number of actinic light steps and adequate replication, within the time required for a single measurement (therefore named 'Single Pulse Light Curve'). This method is illustrated for the generation of LCs of PSII quantum yield ($\Delta F/F_m'$), relative electron transport rate (rETR) and non-photochemical quenching (NPQ), on intact plant leavesexhibiting distinct light responses. This approach makes it also possible to easily characterize the integrated dynamic light response of a sample, by combining the measurement of LCs (actinic light intensity is varied while measuring time is fixed) with induction/relaxation kinetics (actinic light intensity is fixed and the response is followed over time), describing both how the response to light varies with time and how the response kinetics varies with light intensity.

Light-response curves (LC) are widely used in plant physiology for the quantitativedescriptionof the light-dependence of photosynthetic processes (Henley, 1993). Originally developed for characterizing the response of steady state photosynthesis to ambient irradiance (Smith, 1936), LCs attained widespread use following the introduction of Pulse Amplitude Modulated (PAM) fluorometry (Schreiber et al., 1986). Through its ability to monitor the activity of photosystem II (PSII), this technique allows the generation of LCs of relative electron transport rate (rETR;Schreiber et al., 1994), a non-invasive and real-time indicator of photosynthetic activity, shown to be a close proxy for biomass-specific rates of photosynthesis (Genty et al., 1989; Seaton and Walker, 1990). Due to the considerable operational advantages of PAM fluorometry, LCs of rETR became the most common form of quantitatively characterize the light response of photosynthetic activity in plants as well as in virtually all types of photoautotrophic organisms (Rascher et al., 2000; Serôdio et al., 2005; Ye et al., 2012).

Ideally, LCs should be based on independent measurements of the parameter under study. For example, in ^{14}C-based methods of measuring photosynthetic rates in phytoplankton this is the case (Johnson and Sheldon, 2007). It is also possible to generate LCs from PAM measurements in independent replicated samples (Lavaud et al., 2007) but the need to cover a wide range of actinic light levels with appropriate replication makes this approach very time and sample consuming. Therefore, in most cases LCs are generated sequentially, by exposing the same sample to a (usually increasing) range of irradiance levels (Schreiber et al., 1994).

An often overlooked consequence of sequential LCsis that the response of the sample under each light level is strongly affected by its exposure to previous light levels (Perkins et al., 2006; Herlory et al., 2007; Ihnken et al., 2010). LCs constructed in this way are therefore dependent not only on the absolute light levels applied during the generation of the curve but also on the duration of the exposure to each light level and on their order of application. The effects of non-independency between measurements are expected to be intensified in the case of rapid light curves (RLC; Schreiber et al., 1997; White and Critchley, 1999), curves generated by reducing the duration of each light step, normally to just 10-30 s (Rascher et al., 2000; Ralph and Gademann, 2005; Perkins et al., 2006). The short duration of the light steps do not allow the sample to reach a steady state under each light level, thus being largely influenced by previous light history(Serôdio et al., 2006; Ihnken et al., 2010; Lefebvre et al., 2011).

Here we present an alternative method to generateLCs of fluorescence parameters from truly independent, non-sequential measurements. The method is based on the spatial separation of the different levels of actinic light used to construct the light curve, and uses the capabilities of chlorophyll fluorescence imaging systems to simultaneously measure the fluorescence emitted by samples exposed to different irradiance levels. This approach enables light curves to be measured very rapidly, as it only requires that the samples are exposed to the different actinic

light levels for the desired period of time (e.g. to reach a steady-state condition) before a single saturating pulse is applied to measure the fluorescence response of all samples simultaneously. By reducing significantly the time required for the generation of LCs, this approach makes it possible to easily characterize the dynamic light response, by simultaneously tracing the fluorescence response under different light intensities over time.

This work demonstrates the proof of concept for the generation of LCs through the combined use of (i) sample illumination with spatially separated light beams of different intensity, through the use a digital projector as a source of actinic light, and (ii) imagingchlorophyll fluorometry. The application of the method is illustrated for intact plant leaves, but its general principle of operation is applicable to any other type of photosynthetic samples, like macroalgae, lichens or suspensions of microalgae or chloroplasts.

RESULTS

Rationale of the method

The method is based on the illumination of replicated samples with actinic light of different intensities and on the simultaneous detection of the induced fluorescence by an imaging chlorophyll fluorometer. The method requires a number of conditions to be met.

A fundamental requirement is that the illumination of the samples with different levels of actinic light must not interfere with its exposure to the measuring light and saturation pulses. For this reason, the best solution is to project on the samples the required combination of actinic light levels (‘light mask’, see below) using a light source positioned from such a distance that the measuring light and saturating pulses can reach the samples unimpeded. This approach also allows for the measuring light and the saturating pulses to illuminate the sample while it is exposed to the actinic light, a critical condition of the saturating pulse method (Schreiber et al., 1986). Nonetheless, in order to be useful for the generation of a light curve, the fluorescence response must be related solely to the different actinic light levels applied. This implies the use of either replicated samples (e.g. microalgae culture in a multi-well plate) or a homogeneous single sample (e.g. whole leaf). In the latter case, however, the independence of the measurements may be compromised by light scattering within the sample (leaf tissue) causing light spillover between adjacent areas illuminated with different actinic light levels (see below). In this study a digital projector was used as a source of actinic light, due to the large potential advantages deriving from the versatility provided by the digital control of light output. However, the novelty of this approach in plant photophysiology required extensive testing both regarding the emitted light and the detection of fluorescence response.

Regarding light output, the digital projector used in this study was analyzed concerning the spectral characteristics of the emitted light. An important condition for any light source to be used for generating light-response curves is that the light spectrum does not change significantly over the range of light intensities applied. Otherwise, substantial distortions in the light curve shape may be induced, as the photosynthetic light absorption varies significantly along the different regions of the spectrum. This was tested by measuring the spectrum of light emitted at the various output intensities used for generating light curves.

The use of a digital projector was also tested regarding the potential interference on the detection of the fluorescence signals. Images produced by digital projectors are known to suffer from flickering which, although imperceptible to the human eye, may affect the determination of fluorescence levels F_s and F_m' and the calculation of fluorescence indices like $\Delta F/F_m$' or NPQ. Preliminary tests were made on the two main types of digital projector, LCD and DLP projectors. In LCD projectors, images are generated from light beams (three, each of one primary color) passing through separate LCD panels made of a large number of liquid crystals, each corresponding to a pixel in the projected image. The three beams are later combined into a single, full color beam. In the case of DLP technology, the projected light beam arises from light reflected from a reflective surface made of a large number of small mirrors (DLP chip), each corresponding to a pixel in the final image. The orientation of each mirror is controlled individually determining the intensity of each pixel. The interference of actinic light flickering on fluorescence measurements was tested by analyzing the fluorescence kinetics immediately before (determination of F_s level) and during the application of a saturating pulse (determination of F_m' level), on samples exposed to different actinic light intensities provided by the projector. DLP projectors exhibited a much higher intensity of flickering, making them impossible to use in this context. The study was thus carried out using a LCD projector (see below).

Actinic light spectrum

The spectrum of the light emitted by the digital projector covered the wavelength range of PAR, from ca. 430 nm to over 700 nm (Fig. 2A). The projected light was rich in photosynthetically active blue light, its spectrum showing a distinct peak at 440 nm, but poorer in red light (650-700 nm band). The spectrum showed two large peaks in the green-yellow region, centered at 550 and 580 nm. Very little thermal radiation (above 750 nm) was emitted, even when applying the highest PAR levels. This means that the used projectorwas a suitable source of coldactinic light, which did not induce differences in temperature over the different AALs.

The light spectrum was found to change substantially when varying the lamp output intensity (Fig. 2B). Below moderate PAR values (e.g. 580 µmol m^{-2} s^{-1} at the sample level), irradiance increased equally over most of the spectral range (flat spectrum from 440 to 675 nm;

when compared to 150 µmol m^{-2} s^{-1}). But for higher lamp outputs (e.g. 1125 µmol m^{-2} s^{-1}), the spectrum was increasingly enriched in green-yellow light (mainly green, 525-590 nm, and yellow-orange, 600-660 nm) becoming comparatively poorer in photosynthetically active blue and red light. The variation of the light spectrum with intensity may represent a major problem for the generation of light-response curves. Because the yellow-green light that dominates the spectrum when applying higher light levelsis poorly absorbed by photosynthetic pigments, the corresponding values of $\Delta F/F_m$' (or rETR) will appear overestimated when plotted against the measured PAR levels. As a result, rETRlight-response curves may show an inflexion in the light-saturated region, showing an increase of rETR values when stabilizationor even a decrease would be expected.

This problem was addressed by manipulating the spectrum of emitted light so that the proportions of red, green and blue (RGB ratio) regions of the spectrum remained approximately constant over the whole range of light intensities applied.This was achieved through an iterative process of changing the MS Visual Basiccode controlling the RGB ratio of the images produced by the projector, measuringthe emitted spectrum, and calculatingthe resulting proportions of red, green and blue spectral regions. The RGB code allowed to independently controlthe spectral ranges of 400-486 (blue), 487-589 (green-yellow) and 590-690 (red) nm.This procedure was repeated until the same proportions of RGB were obtained in the emitted light for the various PAR levels that were used for generating light-response curves.An average proportion R:G:B of 0.7:2.2:1was used (Fig. 2C), which,by having a higher proportion of yellow-green light ensured the emission of high maximum PAR levels (1125 µmol m^{-2} s^{-1} at the sample level).

Actinic light flickering

The projector light showed noticeable flickering, causing obvious fluctuations in the fluorescence trace (Fig. 3). Light flickering caused interferences at 1.8 s intervals, more pronounced under higher actinic light levels, when it significantly affected the correct determination of both F_s and F_m' levels.Using the data of Fig. 3 as an example, if the full fluorescence record was considered for calculating F_s and F_m', it would result in an underestimation of $\Delta F/F_m$' values of 3.0% and 22.3%, for 260 and 850 µmol m^{-2} s^{-1}, respectively. To avoid these confounding effects it was necessary to analyze the fluorescence recording for each individual measurement (immediately before and during a saturating pulse) and exclude the affected data points.

Application to intact leaves

The method was tested on intact leaves of plants acclimated to different light regimes, expected to show contrasting features in light-response curves of fluorescence. Figure 4 shows

chlorophyll fluorescence images resulting from the application of anactinic light mask to leaves of HL-acclimated *Hedera helix* (Fig. 4A-C) and LL-acclimated *Ficusbenjamina* (Fig. 4D-F)for a known period of time.

Images of F_s andF_m' of *H. helix*(Fig.4A,B) showed some degree of heterogeneity, with higher absolute pixel values in the central region of the leaf, and lower values in the extremities. This was due to the large leaf size in relation to the projected light fieldsof measuring light and saturating pulses. However, this didnot affect significantly the determination of the ratio $\Delta F/F_m$', which remainedrelatively constant throughout the whole leaf (varying between 0.79 and 0.83; Fig. 4C). In the case of *F. benjamina*, although the smaller leaf size helped reduce the effects of light field heterogeneity,spatial variability was still noticeable due to certain leaf anatomical features (e.g. central vein). Again, while this was evident for F_s and F_m' images, the effect mostly disappeared when the ratio $\Delta F/F_m$' was calculated (Fig. 4F).

The application of the actinic light maskon intact leaves resulted in well-defined areasof induced fluorescence response. Particularly for higher light levels, each AAL showed a noticeable outer ring of pixels of intensity intermediate between background values (not illuminated areas) and fully illuminated areas (center of each AAL). The resulting fluorescence images showed a clearly different pattern of response to actinic light in the two plants. Whilst for the HL-acclimated *H. helix*, little effects were observed on F_s, which remained virtually constant over the range of PAR levels applied (Fig. 4A), for the LL-acclimated *F. benjamina*, a large variation in F_s was observed (Fig. 4D). Also regarding F_m', it was clear that in *H. helix*the exposure to high light caused a larger decrease than in *F. benjanima*. As a consequence, clear differences were also observed regarding $\Delta F/F_m$' values, which reached lower values in the LL-acclimated plant.It may be noted that there was a high similarity between replicated AAL and that, as in the case of *F. benjamina*, heterogeneities in F_s and F_m' had little effect on $\Delta F/F_m$' (Fig. 4D-F).

These fluorescence images are also useful to illustrate the variability regarding light scattering within the leaf and its impact on the applicability of the method to intact leaves. *H. helix* leaves showed very low spillover between adjacent AAL, as deduced from the similarity between the pixel values of the areas between AALs and of the background (parts of the leaf distant from AALs; Fig. 4B,C). Notably, larger spillover effectswere observed in the lower (abaxial)surface of the *H. helix* leaves (data not shown). In contrast with *H. helix*, leaves of *F. benjamina* showed a much larger light spillover around AALs. Both for F_s and F_m', the areas around AALs showed pixel values clearlydifferent from the background values (Fig. 4D, E). However, this didnot seem to affect significantly the determination of F_s, F_m' or $\Delta F/F_m$' in each AOI, as no asymmetry was evident in pixel intensity within the AOI of the mask'souter arrays.

Light-response curves: 'Single Pulse Light Curves'

After defining AOIs matching the projected AALs (Fig. 4), the values of F_s and F_m' were determined for the various actinic light levels. These values were used to calculate indices $\Delta F/F_m$', rETR and NPQ that, when plotted against incident actinic light, resulted in light-response curves (Fig. 5). These 'Single Pulse Light Curves' (SPLC),despite requiring just a few minutes of light mask exposure and a single saturating pulse, nevertheless allowed to characterize in detail the light response of the tested samples. Strong indications of the quality of these light curves were the low variability between replicates (measurements on AALs of identical PAR level, corresponding to a same row of the light mask), and the very good fit obtained with well-establishedmathematical models for describing rETR and NPQ vs*E* curves. The light-response patterns were consistent with the ones expected for LL- and HL-acclimation states. Departing from similar F_v/F_m values, $\Delta F/F_m$' decreased more steeplywith increasing irradiance in LL-acclimated *F. benjamina* than in HL-acclimated *H. helix* (Fig. 5B, E). This resulted in distinct rETRvs*E* curves,with *H. helix* showing higher values for initial slope (α) and, mainly, maximum rETR ($rETR_m$, ca. 5 times higher than for *F. benjamina*). Also typical of the difference between LL- and HL-acclimated samples, the photoacclimation indexE_k was much higher (more than double) in *H. helix*than in *F. benjamina*, in accordance with the fact that the former showed little signs of saturation even at 1125 µmol m^{-2} s^{-1}, while the lattersaturated at comparatively lowerPAR values (Fig. 5E).Also in the case of NPQ vs*E* curves, the results were in agreement with expected LL- and HL-acclimation patterns, with *H. helix* reaching higher maximum NPQ values (NPQ_m), requiring higher light levels for full development (E_{50}) and higher sigmoidicity (*n*).

Dynamic light response

A further application of the method concerns the study of the temporal variation of the light response. Figure 6 shows an example of the variation over time of $\Delta F/F_m$' rETR and NPQfor *H. helix* and *F. benjamina*during lightinduction underdifferent PAR levels. Confirming the very different light-response patterns observed before, this approach made it possible to additionally compare the temporal variation of the response of each fluorescence index. For the HL-acclimated *H. helix*, $\Delta F/F_m$' and rETR stabilized quite rapidly, reaching a steady state within 4-6 min upon light exposure (Fig. 6A,C). The patterns of variation were essentially the same for the different light levels, although stabilization was faster for the samples exposed to lower PAR. For NPQ, steady state was reached only after 8-10 min, the induction pattern varying with the light level applied (Fig. 6E).In the case of LL-acclimated *F. benjamina*, all indices took a longer time to reach a steady state (Fig. 6 B,D,F). This was especially true for NPQ, which still increased for most of the PAR levels after 14 min of light exposure.

This approach isalso particularly useful to follow the changes in the light-response curve and to determine the time necessary for reaching of a steady-state. This can be achieved by

following the variation over time of the model parameters used to describe the light-response curves. Using the dataset partially shown on Fig. 6, Fig. 7 shows the variation during light induction of the parameters of rETR and NPQ vs*E*curves. Regarding the rETRvs*E* curves, α was the parameter that showed a smaller variation over time, increasing modestly until reaching stable values after 6 and 10 min for *H. helix* and *F. benjamina*, respectively (Fig. 7A). In contrast, $rETR_m$ and E_k showed much largerfluctuations, particularly for *H. helix*, requiring more than 8-10 min for reaching relatively stable values (Fig. 7B, C).For the parameters of NPQvs*E* curves, similar time periods of 6-10 min were necessary for reaching steady state conditions (Fig. 7 D-F).However, despite the different induction patterns observed for HL-and LL-acclimated samples, most of the differences observed at steady state were already present at the first measurements(2-4 min). This indicates that even a short 2-4 min period of light mask exposure may be sufficient to characterize LCs and detect differences between different light acclimation states.

Light stress-recovery experiments and NPQ components

This approach can be easily extended to carry out light stress-recovery experiments, in which samples are sequentially exposed to high light and then to darkness or low light, and the fluorescence kinetics during light induction and dark relaxation is used to evaluate the operation of photoprotective and photoinhibitory processes (Walters and Horton, 1991; Müller et al., 2001). Usually, only one light level is used, of arbitrarily chosen intensity(Rohácek, 2010; Serôdio et al., 2012).By applying a light mask conveying a range of actinic light it becomes possible to study the fluorescence kinetics during light induction and dark relaxation for different PAR intensities simultaneously.

This is exemplified with the response of NPQ of LL-acclimated *F. benjamina*during light induction and subsequent dark relaxation (Fig. 8).A large and detailed dataset was obtained from a single leaf on the NPQ induction under various PAR levels (Fig. 8A, B) and on its relaxation in the dark (Fig. 8C, D). Figure 8 also highlights the two types of information that can be extracted from the same dataset: light-response curves (Fig. 8A,C) and induction/relaxation kinetics (Fig. 8B,D). By applying the rationale used for the calculation of NPQ components, such a dataset can be used to generate light-response curves of coefficients quantifying photoprotection capacity and susceptibility to photoinhibition(Guadagno et al., 2010). Figure 9 illustrates thisapproach by comparingthe repartition of absorbed light energy in HL-acclimated *H. helix* and LL-acclimated *F. benjamina*. The former plant was shown to be able to use a larger fraction of absorbed light for photochemistry ($\Delta F/F_m'$; ca. 0.5 above 800 µmol m^{-2} s^{-1}; Fig. 9A) while non-photoprotective NPQ components (qT+qI) remained under relatively low values (< 20%) and only started above 400 µmol m^{-2} s^{-1} (Fig. 9A).In contrast, for the LL-acclimated *F. benjamina* $\Delta F/F_m'$ was much lower throughout the light intensity range

(<0.2 for PAR as low as 400 µmol m^{-2} s^{-1}; Fig. 9B) and NPQ started to increase under much lower PAR levels, reaching maximum values at ca. 200 µmol m^{-2} s^{-1}(qT+qI, qC).

DISCUSSION

Method assumptions

The purpose of this study was to demonstrate the proof of principle of the method, starting by identifying and testing the conditions required for its general application. The successful generation of non-sequential LCs using the combination of spatially separated actinic light beams and imaging chlorophyll fluorescence implied the verification of two types of assumptions:(i) assumptions associated to the projection of an actinic light mask and the detection of the induced fluorescence response, and (ii) assumptions related to the use of a digital projector as a source of actinic light for this purpose. These conditions were tested and shown to be verified.

Regarding the projection of the actinic light mask, a very basic assumption of the method was that the samples exposed to different actinic light levels must have essentially the same inherent physiological light response, so that the fluorescence measured in different AALs may be attributed to the different PAR irradiances applied. In a way, this approach is opposed to the traditional use of chlorophyll fluorescence imaging systems: instead of applying a homogeneous actinic light field to study heterogeneous samples, here aheterogeneous actinic light field is applied to study supposedly homogeneous samples. The verification of this condition is mostly dependent of the physiological heterogeneity on the samples. In some cases, as for suspensions of microalgae or chloroplasts, samples can be prepared so that a uniform response can be assured. However, in the case of leaves, it must be previously confirmed that the area to be used for the measurements is homogeneous regarding its photophysiologicalresponses.The here presented results showed that the method can be successfully applied to whole leaves, through careful selection of uniform areas, in order to minimize the potentially confounding effects of within-leaf spatial inhomogeneity.

Another key assumption of the method is the independence of the measurements. This condition can be easily ensured by using optically separated samples, using cell or chloroplast suspensions, or leaf disks in opaque multi well plates impeding the transmission of light between adjacent samples. Potential problems are thus restricted to optically continuous samplessuch as whole leaves, where light spillover from one AAL to another may result in a lack of independence between adjacent AAL. This effect is analogue to the time dependency between consecutive measurements during a sequential light curve. The results of the tests performed on leaves showedthat this effect varied with species and with the leaf optical

properties affecting the amount of internal light scattering. However, they also showed that light spillover can be greatly minimizedthrough adequate design of the actinic light mask (see below).

Regarding the use of digital projectors as actinic light sources, two conditions appeared to be of most importance: the maintenance of a constant spectrum throughout the range of applied irradiances, and the elimination of effects of light flickering on fluorescence measurements. The maintenance of a constant spectrum is important because changes of light spectrum can have substantial effects on $\Delta F/F_m'$, due to the variation of photosynthetic pigments absorptivity over different wavelength ranges.This effect may be observed when comparing rETR light response curves induced by monochromatic light of different colors (Schreiber et al., 2012). In the present case, the enrichment of the green-yellow part of the spectrum is expected to cause and overestimation of $\Delta F/F_m'$, for the measured PAR, because light of these wavelengths are comparatively less absorbed by the dominating pigments such as chlorophyll *a* and *b*, thus inducing a smaller quenching of F_s and F_m'.Therefore, if the light spectrum varies between different AALs, this will likely result in a deformation of the shape of the LC, resulting in an artifactual absence of saturation or decline under high light.As shown here, this problem may be tackled by digitally manipulating the spectrum of the emitted light. Despite some limitations, as only the spectral ranges corresponding to the RGB coding can be manipulated, this approach was shownto suffice to solve the effects of the changes in lamp output spectrum. Nevertheless, the need for this corrective procedure will depend on the magnitude of the induced effects, in turn dependent on the particular experimental and equipment conditionssuch as projector and lamp type, and PAR levels to be used.

The elimination of effects of light flickering is important because light flickering was shown to cause substantial interferences in the fluorescence record, particularly for high actinic light levels, under which the difference between F_s and F_m' is smaller and the error associated to the determination of $\Delta F/F_m'$ is higher. While affected fluorescence values may be easily identified and eliminated from the calculation of F_s and F_m', this requires the possibility to access the raw fluorescence data, which may not be feasible with some PAM fluorometer models or software.

Light mask design

A crucial piece of the proposed experimental approach is the actinic light mask used to project spatially separated areas of actinic light. The light mask used in this study resulted from a large number of preliminary tests on several aspects such as mask shape and dimension, as well as number, size and disposition of the AALs. Its development followed some principles of general applicability in designing light masks for similar studies:

i) Mask dimension. The shape and size of the light mask should consider thesample dimensions as well as the homogeneity of the measuring light and saturating pulse light fields. Smaller masks likely fit better within the zone of homogenous light field sampling area, while they may also help to avoid heterogeneous parts of the sample (e.g. major leaf veins). On the other hand, too small masks may limit both the total number and size of AALs, and, by implying short distances between adjacent AALs, may increase light spillover and compromise the independency of the measurements.

ii) Number of AALs. A large number of AALs allows for a large number of light levels, which is useful for a good characterization of the light resposne, and for replication, reducing variability and increasing precision of parameter estimation. However, the number of AALs possible to accommodate will be limited by total mask size and by the spillover between adjacent AALs. In the present study, it was possible to accommodate 30 AALs, which resulted in a satisfactorily number of data points along the light curve and a good level of replication. By effectively impeding light spillover (e.g. using opaque multi well plates), this number could be significantly increased without increasing light mask size.

iii) AAL distribution pattern. In principle, AALs should be randomly distributed throughout the light mask. This would minimize any systematic effects due to the AAL position within the possibly inhomogeneous measuring light and saturating pulses fields. However, when spillover effects cannot be completely avoided as in the case of whole leaves, better results were found by arranging the AAL along a gradientof light intensity because in a randomized layout there is a high chance of having adjacent AAL of very different light intensities, resulting in substantial spillover and loss of measurement independency. When AALs are distributed along a light intensity gradient, the light intensity of adjacent AALs will be more similar,thus reducing the relative impact on each other.Besides preventing optical spillover, this design will also minimize the potential exchange of light-induced metabolites between adjacent AALs, which could contribute to some degree of non-independency between measurements, especially during long light exposures, as for the study of dynamic light responses (see below). Although this source of measurement dependencycannot be completely excluded for optically continuous samples, its actual interference on the resulting light-response curve can be minimized by decreasing the difference in light levels between AALs next to each other.

iv) AAL size. Large AALs should be used because more pixels will be considered for the estimation of fluorescence parameters, therefore reducingmeasuring errors. This can be of value in the case of samples showing a high physiological heterogeneity. Large AAL are also preferable because the actual area used for calculation of fluorescence parameters (AOI) must be smaller than the maximum diameter of AAL, to avoid the border effects. The light mask used in this study had AALsof the same size and shape, disposed in linear arrays. However, masks may have AAL of different size or shape and arranged in any other way, to better fit specific

aspects of the sample or sample container. For instance, because under higher actinic irradiances a larger error is associated to the measurement of $\Delta F/F_m'$,AAL of higher light levels could be larger, resulting inmore precise measurements due to the higher pixel number.

Single Pulse Light Curves

The here proposed method for the generation of light-response curves presents a number of innovations and significant advantages relatively to conventional approaches. It enables to: (i) obtain non-sequential, temporally-independent fluorescence measurements; (ii) apply a large and variable number of actinic light levels with adequate replication; (iii) generate a whole LC within the time required for a single measurement; (iv) define and control with unprecedented flexibility and ease of use the actinic light levels to be applied.

The considerable reduction of the total time required for the generation of a LC is one of the major advantages of this approach. As all light levels and replicates are measured simultaneously, the total duration of the LC will be essentially determined by the time defined for each individual measurement (e.g. for reaching a steady-state), independently of the number of light levels and replicates.For example, for the case shown in Fig. 5, the whole LC,consisting of 30 measurements (10 light levels x 3 replicates),could be finished after 6 min of light exposure, while it would have required a minimum of 3 hours if each light level/sample was measured separately. This possibility is particularly useful when studying samples showing fast changesin their physiological state, as a response to stressors or changing environmental conditions, or associated to circadian rhythms (Rascher, 2001).

It is generally desirable for LCs to describe steady-state conditions. ‘Steady-state light curves’ are largely independent from transient responses due to recent light history, making it easier to characterize the inherent physiological light response of a sample and to compare different samples. For the samples tested in this study, periods of 4-6 minutes of light mask exposure were enough to ensure a good characterization of the light response, allowing the estimating LC parameters and detecting differences in photoacclimation state. However, the time necessary to reach steady-state conditions depends greatly on the sample physiological state and previous light history. Also, because it is not likely that a steady state is reached at the same time for all actinic light levels, it isnot possible to define a unique protocol for the application of the SPLC. Its application to samples of unknown physiological response should be preceded by the preliminary monitoring of the variation over time of the fluorescence response under the different actinic light levels.

Dynamic light response

The proposed method also enables to incorporate time in the study of the light response. The variation over time of fluorescence indices such as $\Delta F/F_m'$, rETR or NPQ, like their light

induction and dark relaxation kinetics, is of obvious interest for the characterization of the photophysiology of a sample. However, the patterns of variation during induction or relaxation strongly depend on the level of actinic light applied. In this context, the possibility to follow the response to various actinic light levels simultaneously saves time, making it considerably easier to study the variation over time of the light response. This approach allowsto combine two types of studies that are often carried out separately: (i) light-response curves, in which actinic light intensity is varied while the time for measuring a response is arbitrarily fixed; (ii) induction/relaxation kinetics, in which actinic light intensity is arbitrarily fixed and the response is followed over time. It becomes thus possible to easily characterize the dynamic light response of a sample, describing both how the response to light varies with time and how the response kinetics varies with light.

An application of this possibilityis the construction of light-response curves of fluorescence indices that require the comparison of measurements made at different times. This is the case of the coefficients that quantify the partitioning of non-photochemical quenching in photoprotective (rapidly reversible) and photoinhibitory (slowly reversible) components. In most studies, these components are quantified for a single level of actinic light, usually arbitrarily defined to represent a stressful condition. By applying the proposed method, it became possible to easily generate light-response curves of the various quenching coefficients, a task that requires following the NPQ relaxation kinetics after the exposure to various actinic light levels, and that would otherwise be very time consuming.

Limitations

Despite the considerable advantages the here described method offers, there are a number of potential limitations that must be considered. Although the results here presented are specific to the particular projector model used, these general limitations are likely applicable to any other models that share the same technology.

One limitation regards the range of actinic light levels possible to apply. On one hand, it was not possible to obtain complete darkness, the minimum light intensity in the 'dark' AALs being 5 µmol m^{-2} s^{-1}. This was due both to the limitationsof the projector's output contrast and to the unavoidable light scattering originating from the illuminated areas. While this makes it impossible to measure parameters that require dark adaptation, like F_o and F_m, with the projector turned on, it does not affect significantly the construction of LCs, as 5 µmol m^{-2} s^{-1}can be considered sufficiently low for most applications. For the special case of NPQ vs*E* curves, which require the measurement of F_m(in the dark), the best alternative is to cover the projector's lens, and determine F_m before the LC is started.

On the other hand, the maximum light intensity reached at the samples level may also represent a limitation for the construction of LCs. In the case of the setup used in this study, the

maximum value of 1125 µmol m^{-2} s^{-1} can be considered low when compared to the values reached by many commonly used PAM fluorometers, including imaging systems, generally reaching values above 2000 µmol m^{-2} s^{-1}. Nevertheless, the actual limitation caused by the maximum light output will dependon the capacity to cover the relevant range of light intensities for each particular sample. For the plants used in this study, the range of actinic irradiances applied enabled to characterize with adequate detail the light response of the various fluorescence parameters and indices, including the light-saturated part of the curve.

Another potential limitation derives from the relative low sensitivity of imaging chlorophyll fluorometers. These imaging systems are based on CCD sensors which are less sensitive than photodiodes or photomultipliers that equip the most common types of PAM fluorometers. This limits the detection of fluorescence signals, especially under high actinic light, when F_m' is lower and more difficult to discriminate from the F_s level. Accordingly, some manufacturers do not recommend measuring LCs with PAR levelsabove 700 µmol m^{-2} s^{-1} (Imaging-PAM, 2009). This low sensitivity is expected to be overcome by using samples with a high chlorophyll *a* content, but may limit the use of dilute microalgae or chloroplast suspensions.

Further applications

This study aimed to show the main and most immediate applications of the method. Its use was illustrated on intact plant leaves, but it is potentially applicable to many other types of photosynthetic samples, ranging from large plant leaves, lichens,flat corals, macroalgae or algal biofilms (microphytobenthos, periphyton) to phytoplankton or suspensions of microalgae, chloroplasts or thylakoid suspensions, the main limitation being the chlorophyll *a* concentration. The use of optically separated samples, as in multi-well plates, is advantageous because it eliminates light spillover effects and ensures the independence of the measurements.

The results shown here were obtained using light masks with AALs that only differed regarding light intensity. However, the digital control of actinic light opens other possibilities. One is to manipulate the duration of light exposure so that in the same experiment, replicated samples are exposed to different light doses, given by different combinations of light intensity and exposure duration. Also colormay in principle be digitally manipulated and light masks made to incorporate AALs of different spectral composition. This would enable the possibility to compare the spectral responses of fluorescence indices.

A major result of this study is the introduction of digitally controlled illumination as source of actinic light for photophysiological studies involving PAM fluorometry. It provides unprecedented flexibility in the control of the various aspects of projected actinic light field. As this study showed, commercially-available models of digital projectors, used in combination with commonly-available software, may provide a readily accessible and inexpensive way of

applying actinic light mask and generating SPLCs. However, such models were not built for this purpose and their correct use requires some adaptations, namely regarding image flickering and changes in light spectrum. We hope that this study may serve as guidelines for overcoming the limitations of currently available projectors, and to stimulate the development of dedicated equipment.

MATERIAL AND METHODS

Experimental Setup

The setup was comprisedof a combination of aPulse Amplitude Modulation (PAM) imaging chlorophyll fluorometerand a digital projector, used as actinic lightsource (Fig.1). The projector was positioned near the fluorometer's CCD camera, in such a way that the projected light incided on the center of the area monitored by the fluorometer's camera (sampling area), optimizing the detection of the induced chlorophyll fluorescence. The projector was also positioned as vertically as possible (angle of 10º from vertical), to minimize asymmetries in the projected light field, and as close as possible to the sample (ca. 40 cm from the projector lens to the center of the sampling area), to maximize light intensity at the sample level.

Imaging chlorophyll fluorometer

The imaging chlorophyll fluorometer (Open FluorCAM 800-O/1010, Photon Systems Instruments; Brno, Czech Republic) comprised four 13 x 13 cm LED panels emitting red light (emission peak at 621 nm, 40 nm bandwidth) and a 2/3" CCD camera (CCD381) with an F1.2 (2.8-6 mm) objective.Two of the LED panels providedmodulated measuring light (< 0.1 µmol m^{-2} s^{-1}), and the other two provided saturating pulses (>7500 µmol m^{-2} s^{-1}, 0.8 s). Chlorophyll fluorescence images (512 x 512 pixels, 695-780 nm spectral range) were captured and processed using the FluorCam7 software (Photon Systems Instruments; Brno, Czech Republic).When measuring long sequences of fluorescence images (dynamic light response, see below), the Fluorcam7 software was controlled by a AutoHotkey(version 1.1.09.00; available at www.autohotkey.com) script written to automatically run the protocol used for applying saturating pulses, save the fluorescence kinetics data for each measurement and export data as text files for further processing.

Digital projector

All presented results were obtained using a LCD digital projector (EMP-1715, Epson, Japan), comprising a mercury arc lampproviding a light output of 2700 lumens. Afocusing lens was used to focus the projected images in the fluorometer's sampling area. The projected light field covered a rectangular area of ca. 14 x 10 cm.Projector settings were set to provide the widest range of light intensities at the sample level. With the above described setup configuration, PAR levels in the sampling area ranged between 5 and 1125µmol m^{-2} s^{-1}.Actinic PAR irradiance at the sample level was measured using a PAR microsensor (US-SQS/W, Walz; Effeltrich, Germany), calibrated against a recently-calibrated flat PAR quantum sensor (MQ-200, Apogee Instruments; Logan, Utah, USA).

Actinic light mask

The digital projector was used to project anactinic light mask on the sampling area, consisting of a set of spatially separated actinic light areas (AAL), covering the range of PAR levels necessary to induce the fluorescence responses to be used to generate a light curve. The actinic light mask used in this study consisted of 30 circular AALarranged in a 3 x 10 matrix, in which each array of 10 AAL corresponded to 10 different PAR values (5-1125µmol m^{-2} s^{-1}), arranged increasingly so that the highest values were closer to the projector (Fig. 1). Each AAL consisted of a circular homogeneous light field of 4 mm in diameter. Adjacent AALs of the same array were separated by 1.0 mm. Three 10-AAL arrays were projected in parallel (1.5 mm apart) so that approximately the same light levelswere applied on the three arrays. However, due to some unavoidable degree of heterogeneity in the projected light field, a small variation (on average < 2.5%) was presented among replicated AALs.

The light mask was designed in MS PowerPoint, using a code written in MS Visual Basic to define the number, position, size and shape (slightly oval to compensate for the inclination of the projector) of each AAL, as well as the light intensity and spectrum (through controlling the RGB code, see below). This code was used to automatically control the PAR level of each AAL, based on a relationship established between RGB settings and the PAR measured at the sample level.

The chlorophyll fluorescence emitted at each AAL was measured by defining Areas of Interest (AOI) using the FluorCam7 software. The AOIs were centered on the AALs but had a smaller diameter (ca. 3 mm) to minimize border effects that could otherwise introduce significant errors. On average each AOI consisted of 32pixels.

Actinic light spectrum

The spectrum of the light emitted by the digital projector was measured over a 350-1000 nm bandwidth with a spectral resolution of 0.38 nm, using a USB2000 spectrometer (USB2000-VIS-NIR, grating #3, Ocean Optics; Duiven, The Netherlands)(Serôdio et al., 2009). Light was collected using a 400-µm diameter fiber optic (QP400-2-VIS/NIR-BX, OceanOptics)positioned perpendicularly to a reference white panel (WS-1-SL Spectralon Reference Standard, Ocean Optics) placed in the center of the sampling area of the fluorometer and the projected lightfield.A spectrum measured in the dark was subtracted to all measured spectra to account for the dark current noise of the spectrometer. Spectrawere smoothed using a 10-point moving average filter.

Light-response curves

Light-response curves were generated by determining fluorescence parameters F_s and F_m' for each AOI, each corresponding to a different irradiance level. F_s and F_m' were measured by

averaging all pixel values of each AOI andaveraging the fluorescence intensity during the 2 s immediately before the saturating pulse, and during 0.6 s during the application of the saturating pulse (total duration of 800 ms), respectively.The kinetics of fluorescence intensity recorded immediately before and during the application of each saturating pulsewas analyzed for each measurement using the FluorCam7 software, and the parts of the fluorescence trace showing effects of the projector's light flickering were not considered for the estimation of F_s or F_m'. For each AOI (each irradiance level, E), the relative rETR was calculated from the product of E and the PSII effective quantum yield, $\Delta F/F_m'$ (Genty et al., 1990):

$$\mathrm{rETR} = E \frac{F_m' - F_s}{F_m'} = E\, \Delta F \Big/ F_m' \quad (1)$$

Fluorescence measurements were also used to calculate the non-photochemical quenching (NPQ) index, used to quantify the operation of photoprotective and photoinhibitory processes. NPQ was calculated from the relative difference between the maximum fluorescence measured in the dark-adapted state, F_m, and upon exposure to light, F_m':

$$\mathrm{NPQ} = \frac{F_m - F_m'}{F_m'} \quad (2)$$

For each AOI, F_m was measured at the end of a 20 min dark adaptation prior to light exposure. Light-response curves were generated by applying a single saturating pulse after a defined period of light exposure (e.g. 6 min), following a 20 min dark-adaptation period.

Dynamic light response

The potentialities of the method were further tested by characterizing the dynamic light response, i.e. the variation of the fluorescence light response over time. After a 20 min dark adaptation, samples were exposed to the light mask and saturating pulses were applied every 2 min. This rationale was also applied to light stress-recovery experiments, during which samples were subsequentlyexposed to darkness, to allow the characterization of the recovery after exposure to the various actinic light intensities.Data was used to calculate light-response curves and light kinetics (light induction and dark relaxation) of NPQ, as well as the quenching coefficients partitioning NPQ into constitutive, photoprotective, photoinhibitory components, following Guadagno et al. (2010).

Light-response curves models

rETRvs*E* curves were quantitatively described by fitting the model ofEilers&Peeters(1988), and by estimating the parameters α (the initial slope of the curve), $rETR_m$ (maximum rETR) and E_k (the light-saturation parameter):

$$rETR(E) = \frac{E}{aE^2 + bE + c} \quad (3)$$

where

$$\alpha = \frac{1}{c},\ rETR_m = \frac{1}{b + \sqrt{ac}} \text{ and } E_k = \frac{c}{b + \sqrt{ac}} \quad (4)$$

Light-response curves of NPQ were described by fitting the model of Serôdio & Lavaud (2011), and by estimating the parameters NPQ_m (maximum NPQ), E_{50} (irradiance corresponding to half of NPQ_m) and *n* (sigmoidicity parameter):

$$NPQ(E) = NPQ_m \frac{E^n}{E_{50}^n + E^n} \quad (5)$$

The models were fitted using a procedure written in MS Visual Basic and based on MS Excel Solver. Model parameters were estimated iteratively by minimizing a least-squares function, forward differencing, and the default quasi-Newton search method(Serôdio and Lavaud, 2011).

Plant material

The applicability of the method was illustrated on intact plant leaves. To compare the method in samples having distinct light responses, plants acclimated to contrasting light conditions were used.For high-light acclimated plants, leaves of *Hedera helix* L. (common ivy) grown under natural conditions were used. Photoperiod and weather conditions were those of November-December 2012 in Aveiro, Portugal: 10/14 h photoperiod, temperature range of 4-16 ºC, relative humidity of 60-80%, precipitation of 100-200 mm, 95-120 insolation hours. For low-light acclimated plants, leaves of *Ficusbenjamina* L. (weeping fig) grown in a greenhouse during the same time of year were used (average PAR of 20 µmol m^{-2} s^{-1}).All plants were grown in standard horticultural soil, and watered every two days. These two species were selected also to illustrate the variability among leaf optical properties potentially affecting the measuring of fluorescence in closely located illuminated areas (light scattering within the leaf). Unless stated otherwise, all fluorescence measurements were made in the upper (adaxial) surface of the leaves.

List of abbreviations

α - Initial slope of the rETR vs. *E* curve

a, b, c – parameters of the Eilers and Peeters (1988) model

AAL – Areas of Actinic Light

AOI – Areas of interest

$\Delta F/F_m'$ – Effective quantum yield of PSII

E– PAR irradiance (µmol photons m^{-2} s^{-1})

E_{50} – Irradiance level corresponding to 50% of NPQ_m in a NPQ vs. *E* curve

E_k– Light-saturation parameter of the rETR vs. *E* curve

rETR – PSII relative electron transport rate

$rETR_m$ – MaximumrETR in a rETR vs. *E* curve

F_o, F_m – Minimum and maximum fluorescence of a dark-adapted sample

F_s, F_m' – Steady state and maximum fluorescence of a light-adapted sample

F_v/F_m – Maximum quantum yield of PSII

HL – High light

LC – Light-response curve

LL – Low light

n – Sigmoidicity coefficient of the NPQ vs. *E* curve

NPQ – Non-photochemical quenching index

NPQ_m – Maximum NPQ value reached in a NPQ vs. *E* curve

PSII – Photosystem II

Φ_{qC}– quantum yield of chlorophyll photophysical decay

Φ_{qE}–quantum yield of energy-dependent quenching

Φ_{qT+qI} – quantum yield of state transition and photoinhibitory quenching

SPLC – Single Pulse Light Curve

ACKNOWLEDGEMENTS

We thank Gonçalo Simões for invaluable technical help on testing of digital projectors. This work benefited from discussions with Sónia Cruz, Jorge Marques da Silva, Paulo Cartaxana, and David Suggett.

REFERENCES

Eilers PHC, Peeters JCH (1988) A model for the relationship between light intensity and the rate of photosynthesis in phytoplankton. Ecol Model **42**: 199–215

Genty B, Briantais JM, Baker NR (1989)The relationship between the quantum yield of photosynthetic electron transport and quenching of chlorophyll fluorescence. BiochimBiophysActa**990**: 87–92

Genty B, Harbinson J, Baker NR (1990)Relative quantum efficiencies of the two photosystems of leaves in photorespiratory and non-photorespiratory conditions. Plant PhysiolBiochem**28**: 1–10

Guadagno CR, Virzo De Santo a, D'Ambrosio N (2010) A revised energy partitioning approach to assess the yields of non-photochemical quenching components.BiochimBiophysActa**1797**: 525–530

Henley WJ (1993)Measurement and interpretation of photosynthetic light-response curves in algae in the context of photoinhibition and diel changes. J Phycol**29**: 729–739

Herlory O, Richard P, Blanchard GF (2007) Methodology of light response curves: application of chlorophyll fluorescence to microphytobenthic biofilms. Mar Biol**153**: 91–101

Ihnken S, Eggert A, Beardall J (2010) Exposure times in rapid light curves affect photosynthetic parameters in algae. Aquat Bot **93**: 185–194

Imaging-PAM, M-Series Chlorophyll fluorometer, Instrument description and information for users (2009). Heinz Walz GmbH, Effeltrich

Johnson ZI, Sheldon TL (2007)A high-throughput method to measure photosynthesis-irradiance curves of phytoplankton. LimnolOceanogr Meth **5**: 417–424

Lavaud J, Strzepek RF, Kroth PG (2007)Photoprotection capacity differs among diatoms: Possible consequences on the spatial distribution of diatoms related to fluctuations in the underwater light climate. LimnolOceanogr**52**: 1188–1194

Lefebvre S, Mouget J-L, Lavaud J (2011) Duration of rapid light curves for determining the photosynthetic activity of microphytobenthos biofilm *in situ*. Aquat Bot**95:** 1–8

Müller P, Li XP, Niyogi KK (2001)Non-photochemical quenching.A response to excess light energy. Plant Physiol**125**: 1558–1566

Perkins RG, Mouget JL, Lefebvre S, Lavaud J (2006)Light response curve methodology and possible implications in the application of chlorophyll fluorescence to benthic diatoms. Mar Biol**149**: 703–712

Ralph PJ, Gademann R (2005)Rapid light curves: a powerful tool to assess photosynthetic activity. Aquat Bot **82**: 222–237

Rascher U (2001)Spatiotemporal variation of metabolism in a plant circadian rhythm: The biological clock as an assembly of coupled individual oscillators. ProcNatlAcadSci USA **98**: 11801–11805

Rascher U, Liebig M, Lüttge U (2000)Evaluation of instant light-response curves of chlorophyll fluorescence parameters obtained with a portable chlorophyll fluorometer on site in the field. Plant Cell Environ **23**: 1397–1405

Rohácek K (2010)Method for resolution and quantification of components of the non-photochemical quenching (q_N). Photosynth Res **105**: 101–113

Schreiber U, Bilger W, Neubauer(1994)Chlorophyll fluorescence as a nonintrusive indicator for rapid assessment of in vivo photosynthesis.In: ED Shulze, MM Caldwell, eds,Ecophysiology of Photosynthesis. Springer-Verlag, Berlin,pp 49– 70

Schreiber U, Schliwa U, Bilger W (1986) Continuous recordingof photochemical and nonphotochemical chlorophyll fluorescencequenching with a new type of modulation fluorometer. Photosynth Res **10:** 51–62

Schreiber U, Gademann R, Ralph PJ, Larkum AWD (1997)Assessment of photosynthetic performance of *Prochloron* in *Lissoclinum patella* in hospite by chlorophyll fluorescence measurements. Plant Cell Physiol**38**: 945–951

Schreiber U, Klughammer C, Kolbowski J (2012)Assessment of wavelength-dependent parameters of photosynthetic electron transport with a new type of multi-color PAM chlorophyll fluorometer. Photosynth Res **113**: 127–144

Seaton GGR, Walker DA (1990)Chlorophyll fluorescence as a measure of photosynthetic carbon assimilation. Proc Royal SocLond B **242**: 29–35

Serôdio J, Cartaxana P, Coelho H, Vieira S (2009) Effects of chlorophyll fluorescence on the estimation of microphytobenthos biomass using spectral reflectance indices. Rem Sens Environ **113**: 1760–1768

Serôdio J, Ezequiel J, Barnett A, Mouget J, Méléder V, Laviale M, Lavaud J (2012) Efficiency of photoprotection in microphytobenthos: role of vertical migration and the xanthophyll cycle against photoinhibition. AquatMicrobEcol**67**: 161–175

Serôdio J, Lavaud J (2011) A model for describing the light response of the nonphotochemical quenching of chlorophyll fluorescence. Photosynth Res **108**: 61–76

Serôdio J, Vieira S, Cruz S, Barroso F (2005) Short-term variability in the photosynthetic activity of microphytobenthos as detected by measuring rapid light curves using variable fluorescence. Mar Biol**146**: 903–914

Serôdio J, Vieira S, Cruz S, Coelho H (2006) Rapid light-response curves of chlorophyll fluorescence in microalgae: relationship to steady-state light curves and non-photochemical quenching in benthic diatom-dominated assemblages. Photosynth Res **90**: 29–43

Smith EL (1936) Photosynthesis in relation to light and carbon dioxide. ProcNatlAcadSci USA 22: 504–511

Walters RG, Horton P (1991) Resolution of components of non-photochemical chlorophyll fluorescence quenching in barley leaves. Photosynth Res **27**: 121–133

White AJ, Critchley C (1999) Rapid light curves: a new fluorescence method to assess the state of the photosynthetic apparatus. Photosynth Res **59**: 63–72

Ye Z-P, Robakowski P, Suggett DJ (2012) A mechanistic model for the light response of photosynthetic electron transport rate based on light harvesting properties of photosynthetic pigment molecules. Planta**237**: 837-847

Figure legends

Figure 1. Scheme showing the relative position of the digital projector, the imaging chlorophyll fluorometer components (the CCD camera and the LED panels emitting saturating pulses) the sampling area andthe projected actinic light mask (not at scale). For simplicity, two additional LED panels emitting non-actinic, measuring light, positioned perpendicularly to the shown panels, were omitted.Horizontal arrow indicates increasing levels of actinic light in the light mask.

Figure 2. Variation of light spectrum with intensity.A. Spectrum of the light emitted by the digital projector at different output intensities. Numbers represent PAR measured at the sample level (µmol m^{-2} s^{-1}). B. Variation (%) of the light spectrum relatively to the light projecting 150 µmol m^{-2} s^{-1} at the sample level.C. Comparison between the proportion of G:B and R:B for the different PAR levels used for generating light-response curves, before and after spectral correction through manipulation of the RGB code.

Figure3. Effects of digital projector light flickering (arrows) on the recording of chlorophyll fluorescence immediately prior (for the determination of F_s) and during a saturating pulse (for the determination of F_m'), emitted by a sample exposed to actinic light of 260 and 850 µmol m^{-2} s^{-1}. Values normalized to the first measurement.

Figure 4. Example of the application of an actinic light mask on leaves of HL-acclimated *Hedera helix* (A-C) and LL-acclimated *Ficusbenjamina* (D-F).Images (false color scale) of F_s (A,D), F_m' (B,E) and $\Delta F/F_m$' (C,F) measured after 6 min of exposure to the light mask following a period of 20 min in the dark. Fluorescence levels F_s and F_m' normalized to the range of pixel values in each leaf. Scale bar = 1 cm.

Figure 5.'Single pulse light curves'.Fluorescence light-response curves as generated by the exposure to intact leaves of HL-acclimated *Hedera helix* (A-C) and LL-acclimated *Ficusbenjamina* (D-F) to an actinic light mask (data of Fig. 4). Light-response curves (data points) of fluorescence levels F_s and F_m' (A, D), $\Delta F/F_m$' and rETR (B, E), and NPQ (C, F), fitted models (lines)and estimates of model parameters (Eq. 1 and 2, for rETR and NPQ, respectively).

Figure 6. Dynamic light response.Variation over time of the light response of fluorescence indices $\Delta F/F_m$' (A, B), rETR (C, D) and NPQ (E, F). Measurements made under selected PAR levels (numbers) as projected by using an actinic light mask on intact leaves of HL-acclimated

Hedera helix (A, C, E) and LL-acclimated *Ficusbenjamina* (B, D, F) leaves. Light exposure following a 20 min dark exposure. Mean of 3 replicated measurements. Error bars represent ±1 standard error (n=3).

Figure 7. Dynamic light response: light induction of light-response curves.Variation over time of the parameters of the light-response curve of rETR (A-C; parameters of Eq. 1) and NPQ (D-F; parameters of Eq. 2)measure on intact leaves of HL-acclimated *Hedera helix* and LL-acclimated *Ficusbenjamina*upon light exposure following a 20 min dark adaptation.

Figure 8. Dynamic light response: light stress-recovery experiment.3-D representation of the time and light response of NPQ of a LL-acclimated *Ficusbenjamina* leaf, highlighting the variation over time of the light-response curve (A, C) or the light induction and dark relaxation kinetics (B, D). Light exposure following a 20 min dark adaptation.

Figure 9. Dynamic light response: quantum yield of NPQ components.Light response of the quantum yield of NPQ components Φ_C, Φ_E, and Φ_{T+I}, as calculated from the data of a light stress-recovery experiment carried on intact leaves of HL-acclimated *Hedera helix*(A) and LL-acclimated *Ficusbenjamina*(B).

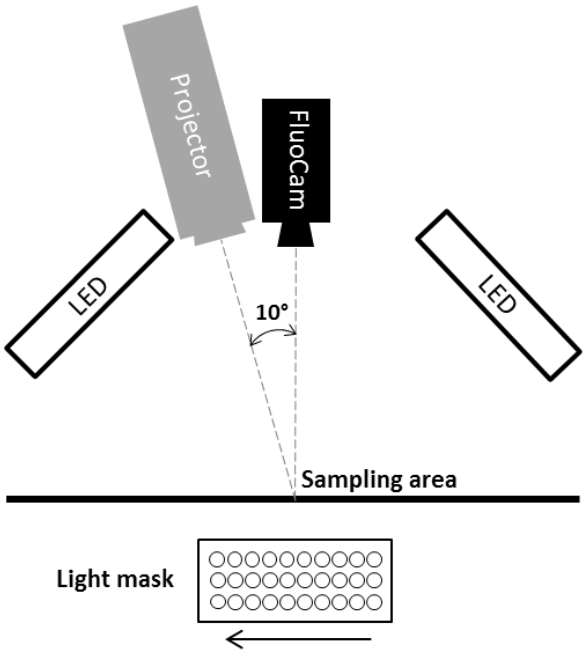

Figure 1. Scheme showing the relative position of the digital projector, the imaging chlorophyll fluorometer components (the CCD camera and the LED panels emitting saturating pulses) the sampling area and the projected actinic light mask (not at scale). For simplicity, two additional LED panels emitting non-actinic, measuring light, positioned perpendicularly to the shown panels, were omitted. Horizontal arrow indicates increasing levels of actinic light in the light mask.

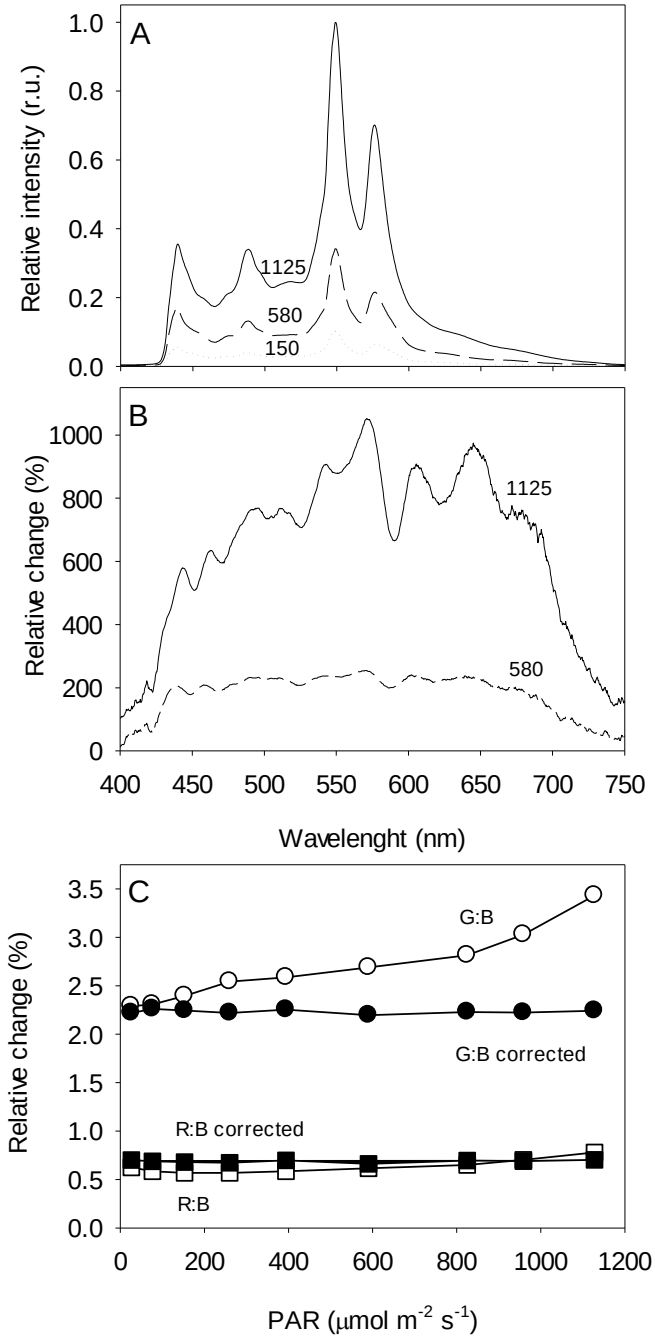

Figure 2. Variation of light spectrum with intensity. A. Spectrum of the light emitted by the digital projector at different output intensities. Numbers represent PAR measured at the sample level (μmol m^{-2} s^{-1}). B. Variation (%) of the light spectrum relatively to the light projecting 150 μmol m^{-2} s^{-1} at the sample level. C. Comparison between the proportion of G:B and R:B for the different PAR levels used for generating light-response curves, before and after spectral correction through manipulation of the RGB code.

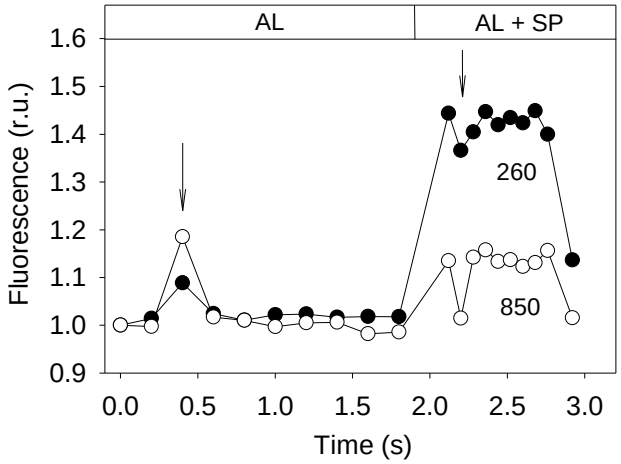

Figure 3. Effects of digital projector light flickering (arrows) on the recording of chlorophyll fluorescence immediately prior (for the determination of F_s) and during a saturating pulse (for the determination of F_m'), emitted by a sample exposed to actinic light of 260 and 850 µmol m^{-2} s^{-1}. Values normalized to the first measurement.

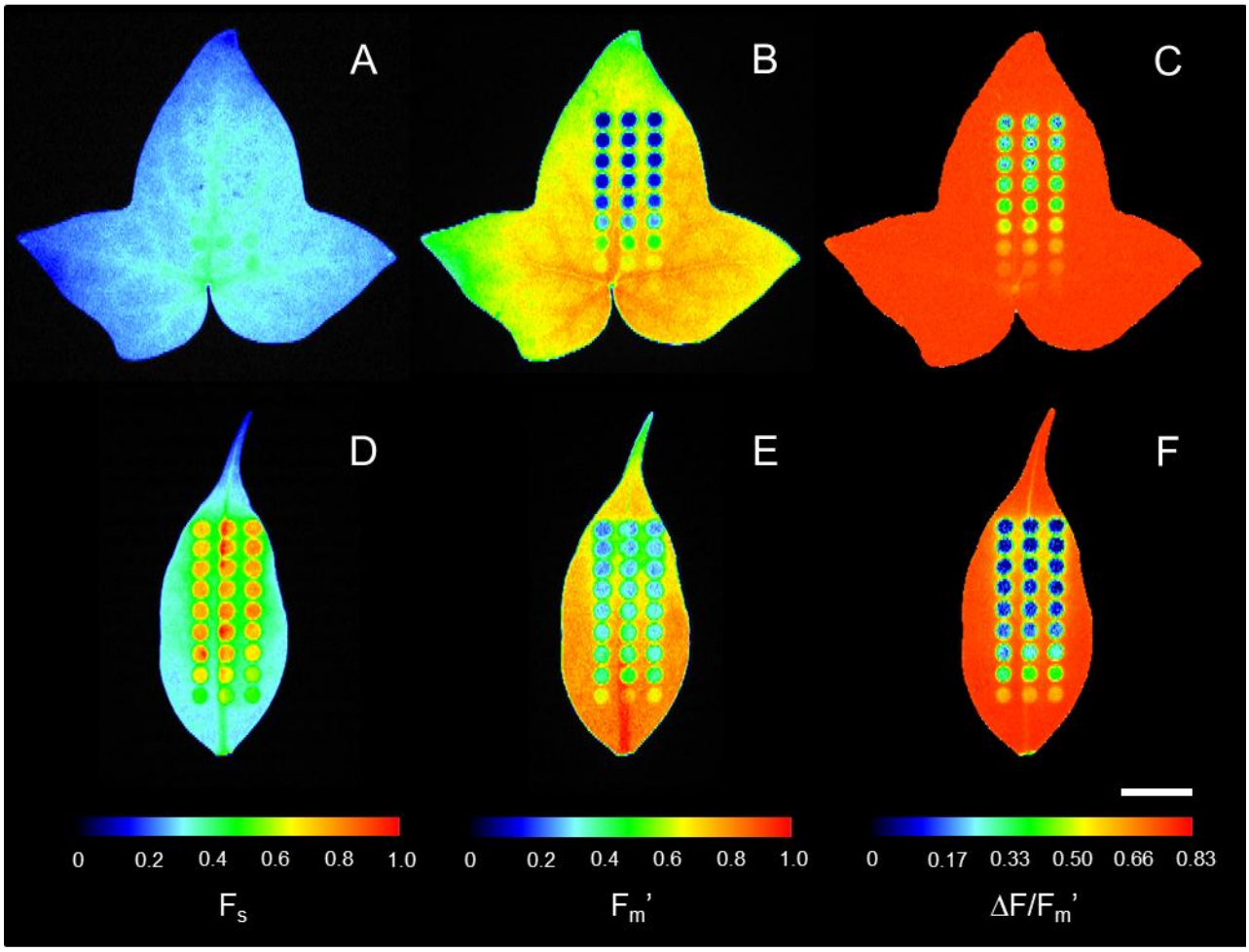

Figure 4. Example of the application of an actinic light mask on leaves of HL-acclimated *Hedera helix* (A-C) and LL-acclimated *Ficusbenjamina* (D-F). Images (false color scale) of F_s (A,D), F_m' (B,E) and $\Delta F/F_m$' (C,F) measured after 6 min of exposure to the light mask following a period of 20 min in the dark. Fluorescence levels F_s and F_m' normalized to the range of pixel values in each leaf. Scale bar = 1 cm.

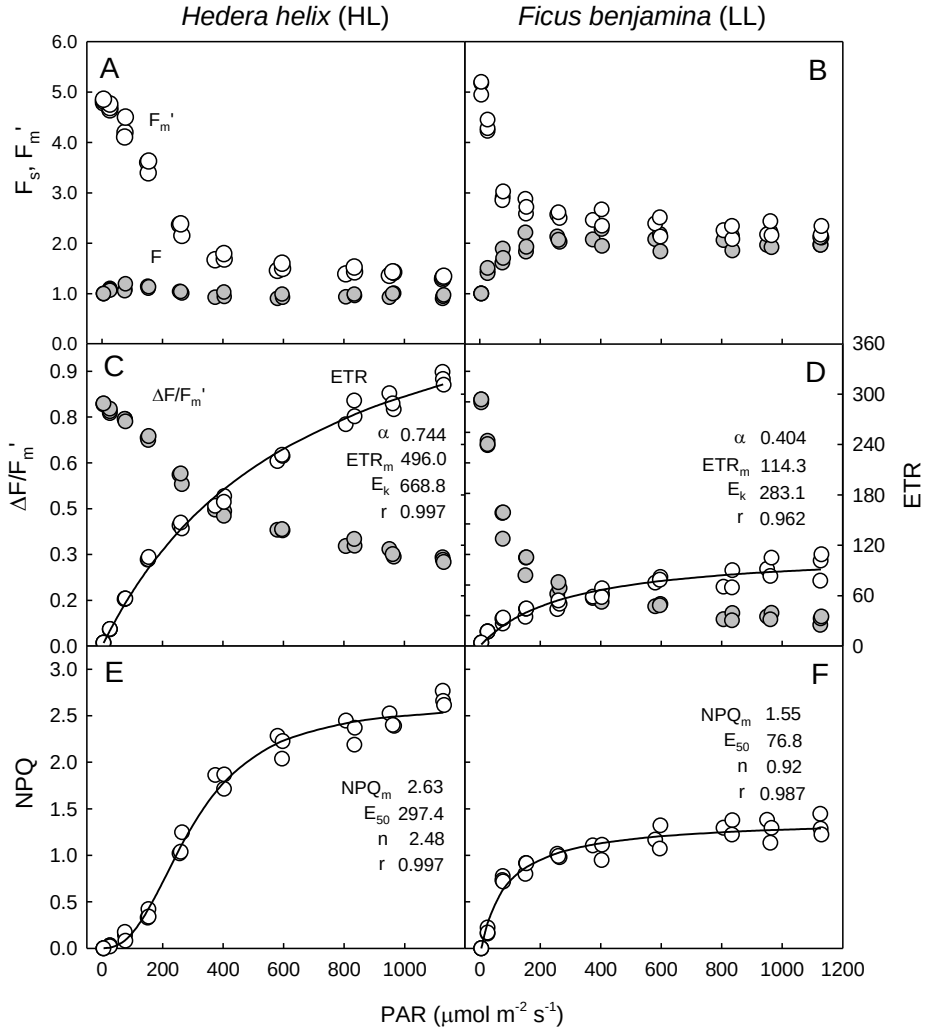

Figure 5.'Single pulse light curves'.Fluorescence light-response curves as generated by the exposure to intact leaves of HL-acclimated *Hedera helix* (A-C) and LL-acclimated *Ficusbenjamina* (D-F) to an actinic light mask (data of Fig. 4). Light-response curves (data points) of fluorescence levels F_s and F_m' (A, D), $\Delta F/F_m$' and rETR (B, E), and NPQ (C, F), fitted models (lines) and estimates of model parameters (Eq. 1 and 2, for rETR and NPQ, respectively).

949

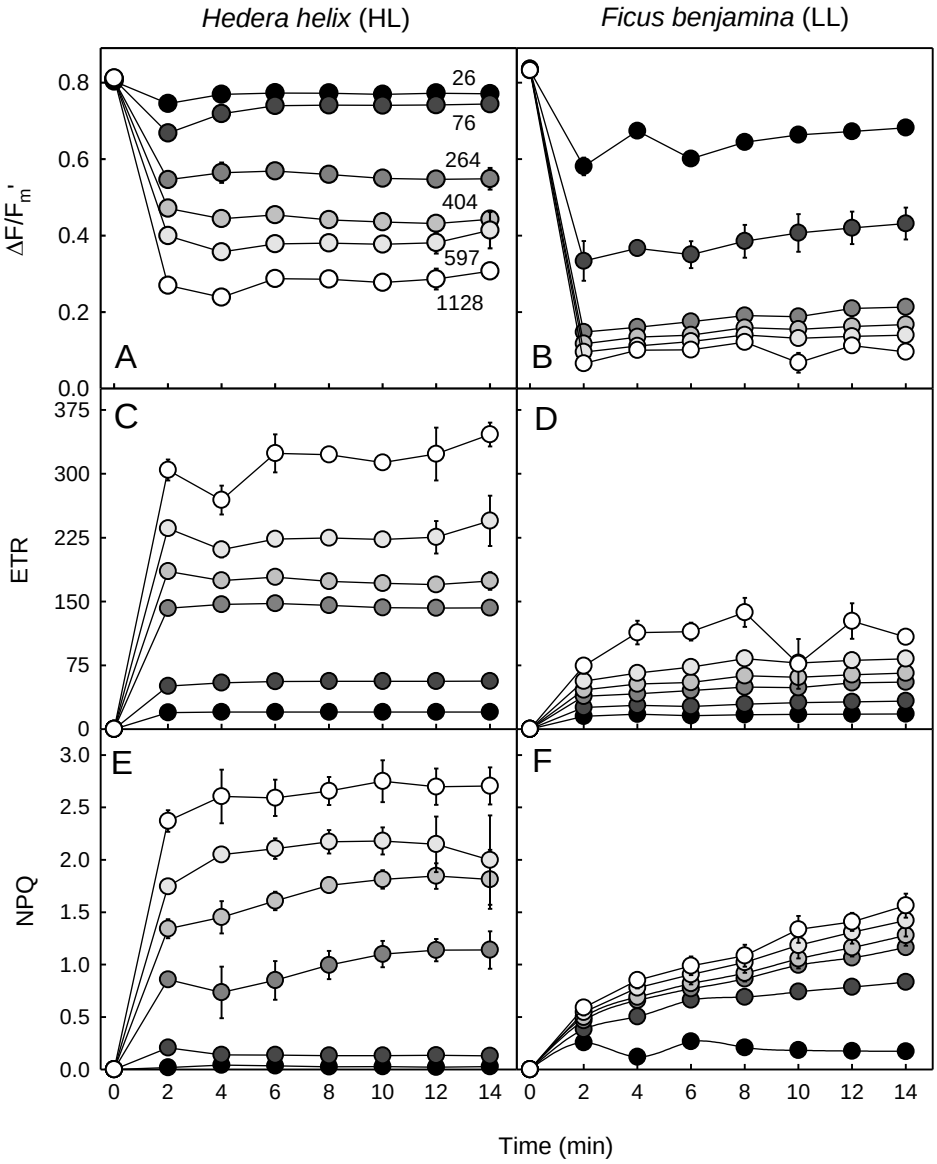

Figure 6. Dynamic light response.Variation over time of the light response of fluorescence indices $\Delta F/F_m$' (A, B), rETR (C, D) and NPQ (E, F). Measurements made under selected PAR levels (numbers) as projected by using an actinic light mask on intact leaves of HL-acclimated *Hedera helix* (A, C, E) and LL-acclimated *Ficusbenjamina* (B, D, F) leaves. Light exposure following a 20 min dark exposure. Mean of 3 replicated measurements. Error bars represent ±1 standard error (n=3).

961
962
963
964

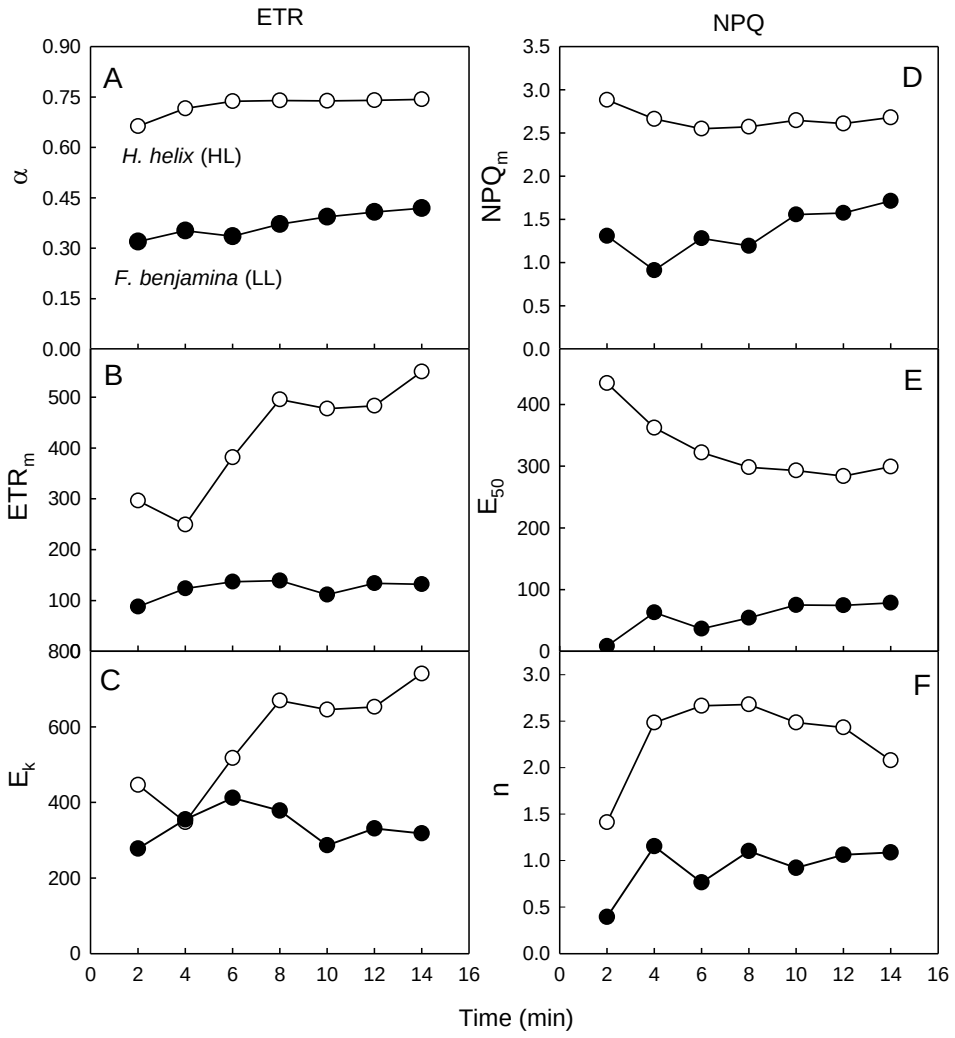

965
966

967 **Figure 7.**Dynamic light response: light induction of light-response curves.Variation over time
968 of the parameters of the light-response curve of rETR (A-C; parameters of Eq. 1) and NPQ (D-
969 F; parameters of Eq. 2) measure on intact leaves of HL-acclimated *Hedera helix* and LL-
970 acclimated *Ficusbenjamina* upon light exposure following a 20 min dark adaptation.
971

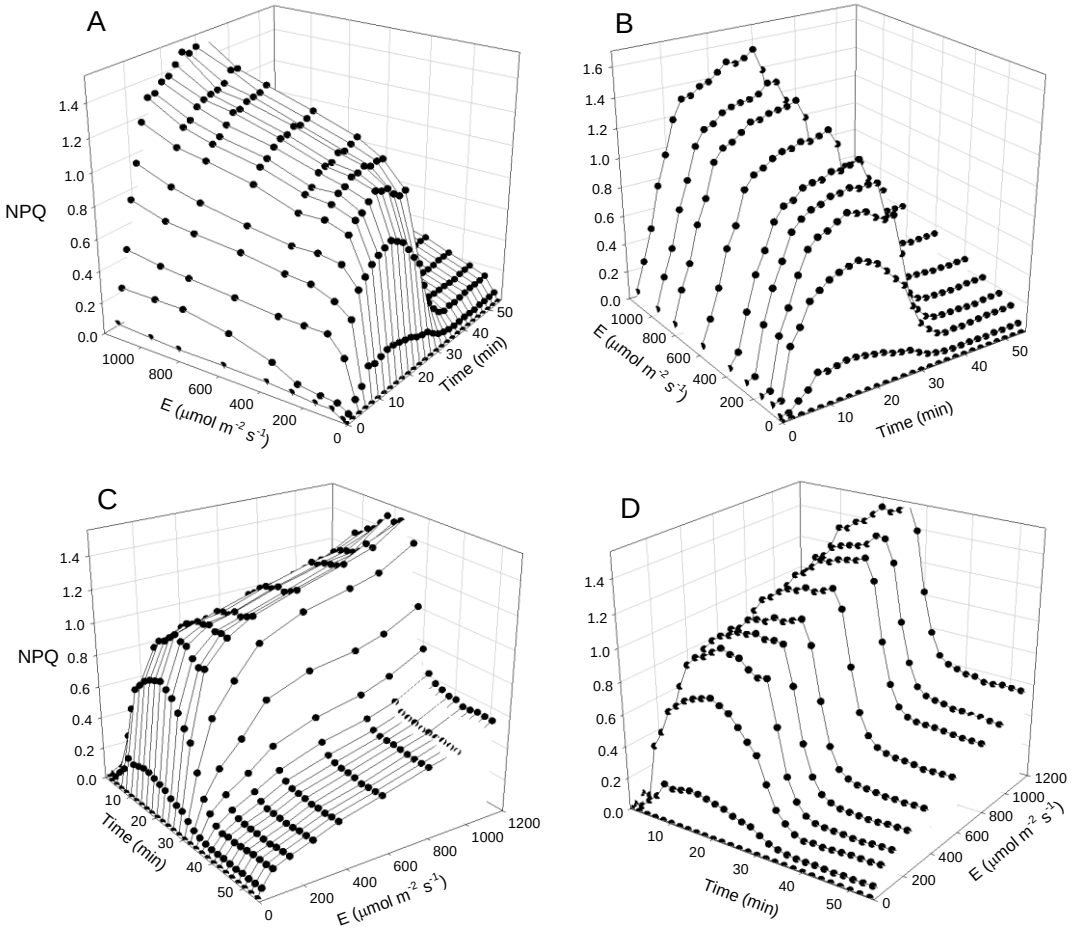

Figure 8. Dynamic light response: light stress-recovery experiment.3-D representation of the time and light response of NPQ of a LL-acclimated *Ficusbenjamina* leaf, highlighting the variation over time of the light-response curve (A, C) or the light induction and dark relaxation kinetics (B, D). Light exposure following a 20 min dark adaptation.

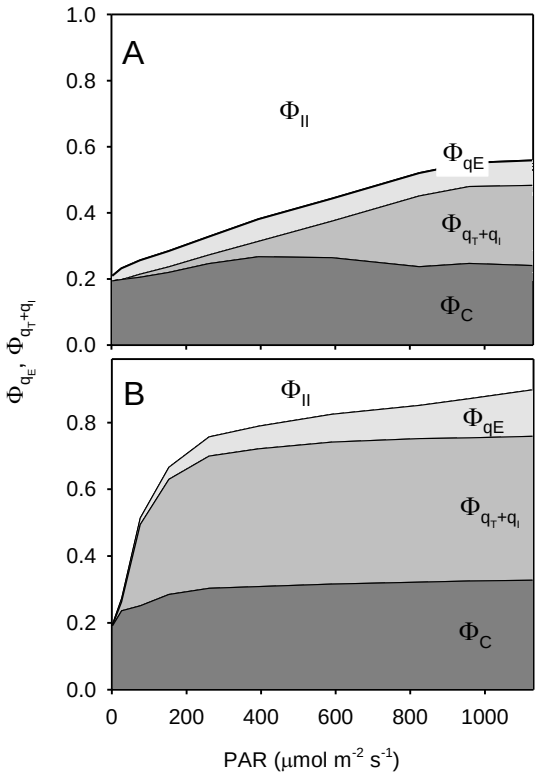

Figure 9. Dynamic light response: quantum yield of NPQ components. Light response of the quantum yield of NPQ components Φ_C, Φ_E, and Φ_{T+I}, as calculated from the data of a light stress-recovery experiment carried on intact leaves of HL-acclimated *Hedera helix*(A) and LL-acclimated *Ficusbenjamina* (B).